Free Rad. Res. Comms., Vol. 3, No. 1-5, pp. 165-172
Photocopying permitted by license only

Printed in Great Britain

DETECTION OF ATMOSPHERIC OH RADICALS

U. PLATT, M. RATEIKE,† W. JUNKERMANN,‡ A. HOFZUMAHAUS and D.H. EHHALT

Kernforschungsanlage Jülich, ICH 3, D-5170 Jülich, W. Germany

(Received July 21st 1986)

The detection of atmospheric OH radicals by laser long path absorption spectroscopy is described. This technique is specific to OH and easily calibrated. In various field measurements from below the detection limit ($5*10^5$/cm^3) up to $8.7*10^6$ OH radicals/cm^3 have been observed. Measurements of meteorologic parameters and mixing ratios of other trace gases simultaneously with OH allow comparison of observed OH levels with reaction kinetic model calculations.

KEY WORDS: OH radicals, spectroscopic measurements, model calculations, laser, atmosphere

INTRODUCTION

The determination of the concentration of free radicals in the atmosphere represents a challenge for the applied experimental techniques. This is particularly true for the detection of OH radicals, since this species is present only at very low concentrations ranging below 10^7 per cm^3 (corresponding to mixing ratios less than 10^{-12}). At the same time in the ambient atmosphere a large number of possibly interfering other trace gases is also present. Thus a useful technique must be very sensitive and highly specific to OH radicals.

During the last decade considerable effort has been made to detect OH radicals in the atmosphere. Nevertheless our experimental knowledge of the distribution of this species is not satisfactory today.

Tracer methods as well as spectroscopic, and chemical techniques have been applied. First, from budget considerations of substances dominantly removed by reaction with OH, its globally averaged concentration can be estimated. Results obtained by observing the budgets of CH_3CCl_3[1-3], CO[4] or ^{14}CO[5] indicate average values around $5*10^5$ OH/cm^3. However, those data do not directly relate to the composition of an individual air mass, therefore in-situ measurements of OH are necessary.

Indirect in situ determinations of OH have been performed by 'spin trapping' atmospheric OH and detecting the resulting complex by electron spin resonance (ESR)[6] or by monitoring its reaction with radioactive ^{14}CO.[7]

To date the majority of the experiments to detect OH radicals in the atmosphere employ spectroscopic techniques. Most spectroscopic methods observe the fluore-

†Present address: Bayer AG, D-5090 Leverkusen.
‡Present address: Frauenhofer Inst. für atmosphärische Umweltforschung, D-8100 Garmisch-Partenkirchen.

scence signal after selectively exciting the OH molecule with laser radiation tuned to an electronic transition of the OH molecule. This 'laser induced fluorescence' (LIF) technique has been used to monitor OH at ground level (see for instance[8–10]) as well as in aircraft ascents.[9,11]

A problem common to all LIF experiments is reliable calibration. A large number of experimental parameters like the geometry of the fluorescence cell or laser output power as well as molecular constants like fluorescence lifetime and quenching efficiencies must be known to relate the observed fluorescence photons to the atmospheric OH concentration. Therefore a field calibration of the apparatus with a known source of OH is usually required.

A more direct spectroscopic approach determines the UV absorption of OH in a long path absorption (LPA) experiment.[12–15] The main advantage of this technique is its inherent calibration, relying only on the absorption cross section of the OH radical, which can be readily derived from laboratory studies.

All above techniques yield OH concentrations from below their detection limits ($\simeq 10^6/cm^3$) up to a few times $10^7/cm^3$. While those data are in general agreement with theory, detailed comparisons are impossible in most cases due to the lack of supporting data like photolysis frequencies and concentrations of other trace gases, which determine the atmospheric OH concentration.

In this paper we describe the technique of laser long path absorption spectroscopy for the detection of OH radicals and present sample results. Simultaneous to the concentration of OH radicals we also measured a comprehensive set of meteorological parameters as well as trace gas mixing ratios. Therefore we are able to compare the measured OH concentrations with model predictions based on the chemical characterisation of the air mass encountered.

EXPERIMENTAL

Our long path absorption spectroscopy (LPA) measurements of OH utilize the strong UV absorption spectrum of the molecule with well resolved rotational lines around 308 nm. The OH lines $Q_1(2)$ and $Q_{21}(2)$ of the $A^2\Sigma^+,\ v' = 0 \leftarrow X^2\Pi_{3/2},\ v'' = 0$ transition were selected for the detection of OH.

As discussed below a broad band light source is tuned to this wavelength region. The light is passed through the free atmosphere, reflected back into the laboratory, and dispersed by a spectrograph. A preselected portion, $\simeq 0.05$ nm wide, of the dispersed spectrum around the OH lines is monitored through repetitive scanning and integration by a fast signal averager. Concentrations of hydroxyl radicals and other air constituents are determined from differential optical absorptions according to Lambert–Beer's law:

$$\ln I_0/I = \sigma * N * l * n/n_0 \tag{1}$$

I	light intensity at the line center
I_0	light intensity at the same wavelength without absorption. This quantity is interpolated from the absorption minima at either side of the absorption line.
σ cm^2	differential absorption cross section at line center
N cm^{-3}	number density averaged along the light path
l cm	length of lightpath

n/n_0 population (n) of the molecular level from which the absorption transition originates compared to the total number (n_0) of molecules.

Since at ambient temperatures several rotational levels of the OH radical are populated, n/n_0 for any particular level is smaller than unity. For one level of the Lambda doublet $X^2\Pi_{3/2}$, $v'' = 0$, $N'' = 2$, $J'' = 5/2$ (lower state of the $Q_1(2)$ and $Q_{21}(2)$ transition used in our experiment) n/n_0 is 0.1 at 293 K.

All factors in equation (1) which relates the observed signal I/I_0 to the desired number density of OH are either measured directly like the pathlength, l, or can be calculated unambiguously from literature data.

The apparent absorption cross section is calculated using the well-known equation (2):

$$\sigma = \pi * r * f * 1/\Delta\nu * 1/a \tag{2}$$

r classical electron radius, $e^2/mc^2 = 2.82 * 10^{-13}$ cm
f oscillator strength
$\Delta\nu$ line width (full width at half maximum, FWHM) cm^{-1}
a shape factor of the absorption line
Gaussian shape (= 1.06), Lorentz broadening (= 1.57).

Literature values for the oscillator strength f for the appropriate line transitions agree within $\pm 10\%$. Here a value of $f = 7.3 * 10^{-4}$ is derived from the Einstein coefficients calculated by Goldman and Gillis,[16] which are based on the lifetime measurements by German.[17]

A fully resolved rotational absorption line of this OH transition in air at 1 atm shows a Voigt profile[18] with $\Delta\nu = 0.18\,cm^{-1}$ as a result of folding a Doppler broadened line profile (Gaussian shape) and a collision broadened line profile (Lorentzian shape).[19] Accordingly the line shape factor would fall somewhere in between the limits given above. However, in our measurements the lines are broadened by experimental effects, which results in an almost Gaussian profile of the OH absorption lines. Consequently $a = 1.06$ was assumed, corresponding to an absorption cross section $\sigma = 6.1 * 10^{-16} * 1/\Delta\nu\ cm^2$.

The experimental details are shown in Figure 1 and are described in the following.

The light source consists of a laser system which emits a spectrally smooth light profile of about 0.1 nm FWHM at 308 nm. This is considerably broader than the sharp absorption features of OH and also wider than the total spectral region scanned around the OH lines. The UV light is obtained by extra cavity frequency doubling the output of a jet stream dye laser. Rhodamin 6G in ethylene glycol is pumped synchronously by the 514.5 nm line (average power about 3 W) from an acousto-optically modulated Argon ion (Ar^+) laser. The pulse frequency is 246 MHz and the width of a single Ar^+ laser pulse about 200 psec. The red dye laser light is focussed into a $LiIO_3$ single crystal for frequency doubling. The average UV power was measured to be 10 to 20 mW. The visible light is blocked off by a dielectric mirror in conjunction with a colour glass filter (Schott UG 5). The pulse duration of the dye laser is a few psec. However for the electronic detection system the light appears to be continuous due to the time constant of the arrangement.

For field measurements a Cassegrain type telescope expands the small diameter of the original laser beam by a factor of 50 to about 0.25 m diameter in order to reduce the divergence of the beam as well as its mean photon flux density. The light is passed into the open atmosphere and reflected by a flat mirror at a distance of 1.5–5.8 Km. A spherical mirror (0.3 m diameter, 2.4 m focal length) focusses the returning light

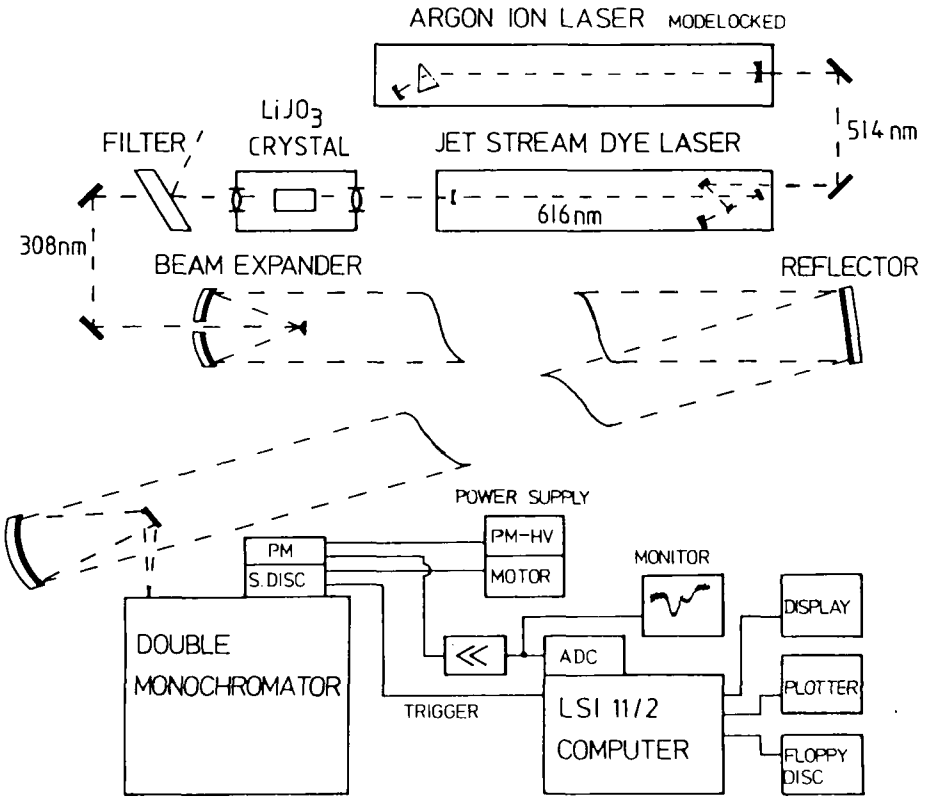

FIGURE 1 Laser light source and receiving system for long path absorption measurements of atmospheric OH radicals. Light path lengths in the open atmosphere range from 3 to 11.6 Km according to local possibilities and desired sensitivity.

onto the entrance slit of a double monochromator operated in second order (Spex 1402; gratings: 2160 grooves mm^{-1}, blazed for 500 nm; dispersion 0.13 nm mm^{-1}; resolution for 10 μm slits based on manufacturers data is estimated to 0.0015 nm FWHM). The single exit slit is replaced by a metal disc (200 mm diameter), which carries 1092 radial slits around its periphery. The slits (10 μm wide, 10 mm long) start 2 mm from the rim and are spaced at $\simeq$ 0.5 mm distance. By rotating the disc a preselected spectral region is scanned by each slit. A stationary mask with a slightly narrower opening than the slit spacing (0.45 mm equivalent to a wavelength interval of 0.058 nm) insures that light passes only through one slit at a time. A single scan takes about 150 μsec corresponding to a repetition rate of 6.6 KHz. The light passing through the scanning slit is recorded by a photomultiplier (EMI 9750QB).

In this way the wavelength dependend intensity distribution of the light is converted into a time varying electrical signal which is fed into an 12-bit analog to digital converter. Synchronization of the mechanical spectrum scan and the data acquisition system is obtained by a light barrier located at the starting edge of the stationary mask. IR-light passes through the slit at the same radial distance as the laser light. During a scan 184 readings are taken at 0.8 μsec time intervals. Each time interval

TABLE I
OH measurement campaigns performed by Laser LPA

Year	Site	Length of light path Km	Range of OH concentration $10^6\,cm^{-3}$
1979	Jülich	3/7.8	1.2–2.2†
1980	Jülich	3/7.8	0.7–2.6 (< 4)
1980	Deuselbach	6/9.7	< 0.5– < 4
1981	Deuselbach	8.6/9.7	< 0.6–4
1982	Jülich	11.6	< 0.7– < 1.6
1983	Deuselbach	9.7	0.7–3.2
1984	Schauinsland	8.6	< 0.5–8.7

†Monthly averages only.

covers 66 pulses of the mode locked laser. The 184 portions of the spectrum are added into the same number of channels of a fast signal averager, and are transferred to a microcomputer (PDP 11, Digital Equipment) for data processing and storage.

The resulting spectral resolution is regularly checked by observing the line pair at 313.155 and 313.183 nm of a mercury low pressure lamp. The resolution was found to be about 0.0027 nm due to jitter of the line position, thus the actual linewidth is

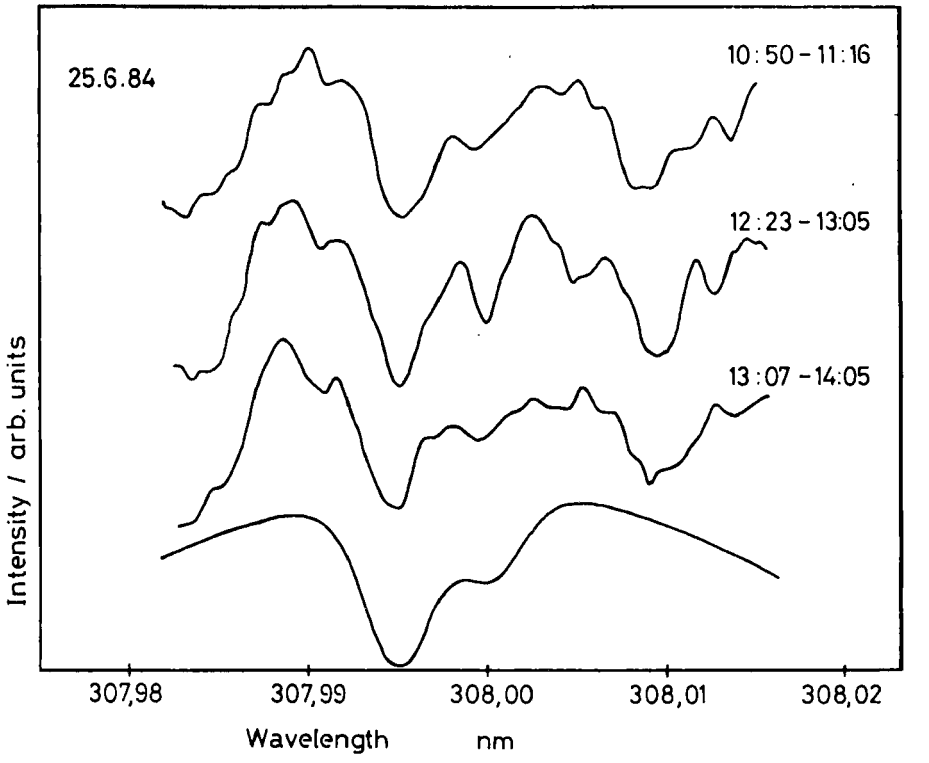

FIGURE 2 Absorption spectra of the OH radical around 308 nm, $Q_1(2)$ and $Q_{21}(2)$ lines of the $A^2\Sigma^+$, $v' = 0 \leftarrow X^2\Pi$, $v'' = 0$ transition are shown. The spectra have been taken in the Black Forest, June 25, 1984, using 8.6 km light path length.

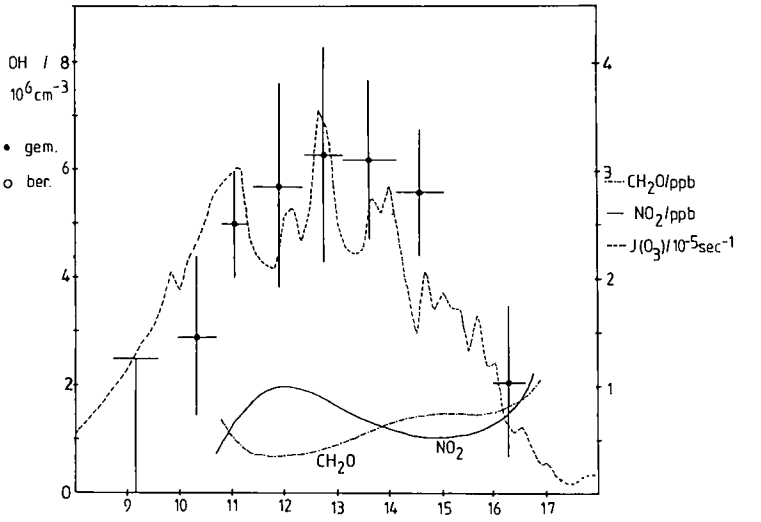

FIGURE 3 Diurnal profiles of OH (crosses), NO_2 (drawn line), CH_2O (dashed/dotted line), and Ozone photolysis frequency (dashed line) at June 25, 1984. Horizontal bars of the crosses indicate averaging intervals, vertical bars give 1σ errors of the OH measurements.

derived from the observed spectra. In field experiments the resolution is also controlled from time to time by calibration with a known absorption spectra, for example of SO_2.

FIELD EXPERIMENTS AND RESULTS

During the last years the technique described has been applied in a series of field campaigns. Three sites covering a wide range of pollution levels were chosen: Jülich (polluted), Deuselbach/Hunsrück (moderately polluted), and Schauinsland/Schwarzwald (slightly polluted). Ultraviolet absorption spectra of atmospheric OH radicals could be identified definitely, with OH concentrations ranging from $< 0.5 * 10^6$ to $8.7 * 10^6/cm^3$. Simultaneously with most OH measurements the concentrations of NO_2, O_3, CH_2O, and SO_2 were also observed by a second LPA apparatus[20,21] using a Xe-arc light source. Table I gives an overview of the campaigns performed and the ranges of OH concentrations encountered. Sample absorption spectra clearly showing two OH lines ($Q_1(2)$ and $Q_{21}(2)$ lines of the $A^2\Sigma^+, v' = 0 \leftarrow X^2\Pi, v'' = 0$ transition) are shown in Figure 2. The lowest trace in Figure 2 gives an OH reference spectrum used as wavelength reference, it is obtained by passing the laser light through a acetylene/air flame. Due to the high temperature the lines are broadened compared to the atmospheric lines. Figure 3 shows diurnal profiles of OH, NO_2, and CH_2O measured at June 25, 1984. The observed OH concentration follows the intensity of the solar UV radiation (dashed line: $J(O_3)$), which initiates photochemical OH formation.[22]

Obviously it is interesting to compare the measured OH concentrations with the values expected from photochemical theory. Therefore calculations of the reaction kinetics related to OH were performed using a 'box model'. The 'auxiliary' data

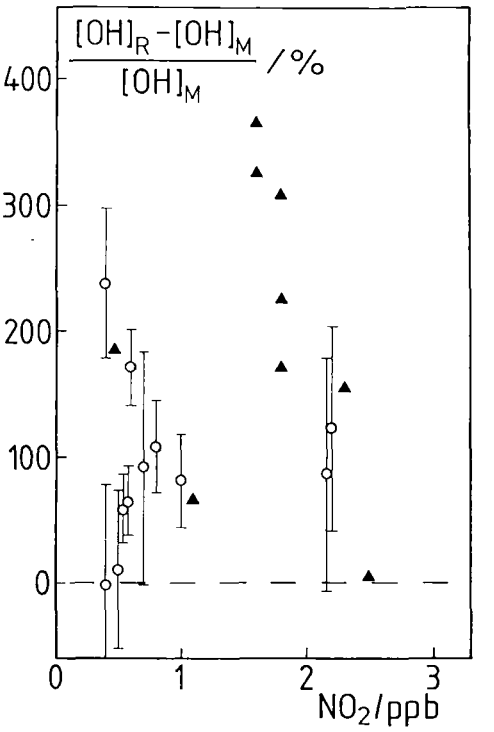

FIGURE 4 Comparison of OH radical concentrations measured $[OH]_R$ in the Black Forest (June, 1984) with model prediction $[OH]_M$ based on auxiliary measurements (UV-flux, mixing ratios of O_3, NO_2, SO_2, CH_2O, water vapour, and light hydrocarbons).

(UV-flux, mixing ratios of O_3, NO_2, SO_2, CH_2O, water vapour, and light hydrocarbons) measured during the time of the OH measurements were used as input parameters. Since OH radicals reach their photochemical steady state concentration within less than a minute transport phenomena play no role and such a comparison of model and measurement should represent a meaningful test of the correctness of the reaction scheme related to OH. While the dependence of the OH concentration on the solar UV intensity is as expected (see Figure 3), the model predicts much larger OH concentrations (up to 3.6 times, see Figure 4) than actually observed, in no case measured values are smaller than predicted.

The reasons for that discrepancy are not clear, possible explanations include deficiencies in the reaction system used to model OH or unknown, possibly heterogeneous, losses of radicals.[23]

References

1. Lovelock, J.E., *Nature*, **267**, 32 (1977).
2. Neely, W.B. and Plonka, J.H. *Environ. Sci. Technol.*, **12**, 317–321, (1978).
3. Singh, H.B., Salas, L.J., Shigeishi, H. and Scribner, E. *Science*, **203**, 899–903, (1979).
4. Hanst, P.L., Spence, J.W. and Edney, E.O. *Atmos. Environ.*, **14**, 1077–1088, (1980).
5. Volz, A., Ehhalt, D.H. and Derwent, R.G. *J. Geophys. Res.*, **86**, 5163–5171, (1981).

6. Watanabe, T., Yoshida, M., Fujiwara, S., Abe, K., Onoe, A., Hirota, M. and Igarashi, S. *Anal. Chem.*, **54,** 2470–2474, (1982).
7. Campbell, M.J., Sheppard, J.C., Hopper, F.J. and Hardy, R. 2nd Symp. Compos. Nonurban Trop., May, 25–28, Williamsburg, Va., AMS, AGU, NASA, 314, (1982).
8. Wang, C.C., Davis, L.I., Wu, C.H., Japar, S., Niki, H. and Weinstock, B. *Science,* **189,** 797–800, (1975).
9. Davis, L.I., Guo, C., James, J.V., Morris, P.T., Postiff, R. and Wang, C.C. *J. Geophys. Res.*, **90,** 12835–12842, (1985).
10. Hard, T.M., O'Brien, R.J., Chan, C.Y. and Mehrabzadeh, A.A. *Environ. Sci. Technol.* **18,** 768–777, (1984).
11. Rodgers, M.O., Bradshaw, J.D., Sandholm, S.T., KeSheng, S. and Davis, D.D. *J. Geophys. Res.*, **90,** 12819–12834, (1985).
12. Perner, D., Ehhalt, D.H., Paetz, H.W., Platt, U., Roeth, E.P. and Volz, A. *Geophys. Res. Lett.*, **3,** 466–468, (1976).
13. Hübler, G., Perner, D., Platt, U., Toennissen, A. and Ehhalt, D.H. *J. Geophys. Res.*, **89,** 1309–1319, (1984).
14. Ortgies, G. and Comes, F.J. *Appl. Phys.* **B33,** 103–113, (1984).
15. Zellner, R. and Haegele, J. *Optics and Laser Technology,* **4,** 79–82, (1985).
16. Goldman, A. and Gillis, J.R. *J. Quant. Spectrosc. Radiat. Transf.*, **25,** 111–135, (1981).
17. German, K.R. *J. Chem. Phys.*, **62,** 2584–2587, (1975).
18. Engleman, R. J. *Quant. Spectrosc. Radiat. Transf.*, **9,** 391–400, (1969).
19. Bakalyar, D.M., James, J.V., and Wang, C.C. *Appl. Optics,* **21,** 2901–2905, (1982).
20. Platt, U. and Perner, D. Measurements of atmospheric trace gases by long path differential UV/visible absorption spectroscopy: Optical and Laser Remote Sensing, D.K. Killinger and A. Mooradian (Eds.) Springer Ser. *Optical Sci.*, **39,** 95–105, (1983).
21. Platt, U. and Perner, D. Ein Instrument zur spektroskopischen Spurenstoffmessung in der Atmosphaere, Fresenius, *Z. Anal. Chem.* **317,** 309–313, (1984).
22. Ehhalt, D.H., Free Radicals in the Atmosphere, this volume (1986).
23. Perner, D., Platt, U., Trainer, M., Hübler, G., Drummond, J.W., Junkermann, W., Rudolph, J., Schubert, B., Volz, A., Ehhalt, D.H., Rumpel, K.J., Helas, G., Tropospheric OH concentrations: A comparison of field data with model predictions, *J. Atmosph. Chem.*, in press, 1987.

Accepted by Prof. H. Sies